REPORT DOCUMENTATION PAGE

Form Approved
OMB No. 0704-0188

PLEASE DO NOT RETURN YOUR FORM TO THE ABOVE ADDRESS.

1. REPORT DATE *(DD-MM-YYYY)*	2. REPORT TYPE	3. DATES COVERED *(From - To)*
	Journal Paper	

4. TITLE AND SUBTITLE

Effects of Surface Treatment and Interfacial Strength on the Damage Propagation in Layered Transparent Armor Under Impact
---Dynamic Ring-On-Ring for Rates and Surface Conditions on Equi-axial Flexural Strength of Brittle Materials

5a. CONTRACT NUMBER

54666EG

5b. GRANT NUMBER

W911NF0810533

5c. PROGRAM ELEMENT NUMBER

6. AUTHOR(S)

Weinong Wayne Chen

5d. PROJECT NUMBER

5e. TASK NUMBER

5f. WORK UNIT NUMBER

7. PERFORMING ORGANIZATION NAME(S) AND ADDRESS(ES)

Purdue University
Sponsored Programs Services
West Lafayette, IN 47907-2108

8. PERFORMING ORGANIZATION REPORT NUMBER

9. SPONSORING/MONITORING AGENCY NAME(S) AND ADDRESS(ES)

Dr. Ralph Anthenien
U.S. Army Research Office
P.O. Box 12211
Research Triangle Park, NC 27709-2211

10. SPONSOR/MONITOR'S ACRONYM(S)

ARO

11. SPONSOR/MONITOR'S REPORT NUMBER(S)

54666EG

12. DISTRIBUTION/AVAILABILITY STATEMENT

Approved for public release; federal purpose rights.

13. SUPPLEMENTARY NOTES

14. ABSTRACT

A novel dynamic ring-on-ring equibiaxial flexural testing technique with single pulse loading capability is established on a modified Kolsky bar. This technique is then utilized to investigate the loading-rate and surface-condition effects on the flexural strength of a borosilicate glass. Quasi-static and dynamic experiments are performed at loading rates ranging from 5x10^-1 to 5x10^6 MPa/s. It is found that the flexural strength of the borosilicate glass strongly depends on the applied loading rates. HF acid corrosion on the surface promotes the flexural strength to above 1.3 GPa. Fractographic analysis shows that surface modification has changed the type of flaws that govern the flexural strength of glass samples.

15. SUBJECT TERMS

16. SECURITY CLASSIFICATION OF:			17. LIMITATION OF ABSTRACT	18. NUMBER OF PAGES	19a. NAME OF RESPONSIBLE PERSON
a. REPORT	b. ABSTRACT	c. THIS PAGE			19b. TELEPHONE NUMBER *(Include area code)*

Reset

INSTRUCTIONS FOR COMPLETING SF 298

1. REPORT DATE. Full publication date, including day, month, if available. Must cite at least the year and be Year 2000 compliant, e.g. 30-06-1998; xx-06-1998; xx-xx-1998.

2. REPORT TYPE. State the type of report, such as final, technical, interim, memorandum, master's thesis, progress, quarterly, research, special, group study, etc.

3. DATES COVERED. Indicate the time during which the work was performed and the report was written, e.g., Jun 1997 - Jun 1998; 1-10 Jun 1996; May - Nov 1998; Nov 1998.

4. TITLE. Enter title and subtitle with volume number and part number, if applicable. On classified documents, enter the title classification in parentheses.

5a. CONTRACT NUMBER. Enter all contract numbers as they appear in the report, e.g. F33615-86-C-5169.

5b. GRANT NUMBER. Enter all grant numbers as they appear in the report, e.g. AFOSR-82-1234.

5c. PROGRAM ELEMENT NUMBER. Enter all program element numbers as they appear in the report, e.g. 61101A.

5d. PROJECT NUMBER. Enter all project numbers as they appear in the report, e.g. 1F665702D1257; ILIR.

5e. TASK NUMBER. Enter all task numbers as they appear in the report, e.g. 05; RF0330201; T4112.

5f. WORK UNIT NUMBER. Enter all work unit numbers as they appear in the report, e.g. 001; AFAPL30480105.

6. AUTHOR(S). Enter name(s) of person(s) responsible for writing the report, performing the research, or credited with the content of the report. The form of entry is the last name, first name, middle initial, and additional qualifiers separated by commas, e.g. Smith, Richard, J, Jr.

7. PERFORMING ORGANIZATION NAME(S) AND ADDRESS(ES). Self-explanatory.

8. PERFORMING ORGANIZATION REPORT NUMBER. Enter all unique alphanumeric report numbers assigned by the performing organization, e.g. BRL-1234; AFWL-TR-85-4017-Vol-21-PT-2.

9. SPONSORING/MONITORING AGENCY NAME(S) AND ADDRESS(ES). Enter the name and address of the organization(s) financially responsible for and monitoring the work.

10. SPONSOR/MONITOR'S ACRONYM(S). Enter, if available, e.g. BRL, ARDEC, NADC.

11. SPONSOR/MONITOR'S REPORT NUMBER(S). Enter report number as assigned by the sponsoring/ monitoring agency, if available, e.g. BRL-TR-829; -215.

12. DISTRIBUTION/AVAILABILITY STATEMENT. Use agency-mandated availability statements to indicate the public availability or distribution limitations of the report. If additional limitations/ restrictions or special markings are indicated, follow agency authorization procedures, e.g. RD/FRD, PROPIN, ITAR, etc. Include copyright information.

13. SUPPLEMENTARY NOTES. Enter information not included elsewhere such as: prepared in cooperation with; translation of; report supersedes; old edition number, etc.

14. ABSTRACT. A brief (approximately 200 words) factual summary of the most significant information.

15. SUBJECT TERMS. Key words or phrases identifying major concepts in the report.

16. SECURITY CLASSIFICATION. Enter security classification in accordance with security classification regulations, e.g. U, C, S, etc. If this form contains classified information, stamp classification level on the top and bottom of this page.

17. LIMITATION OF ABSTRACT. This block must be completed to assign a distribution limitation to the abstract. Enter UU (Unclassified Unlimited) or SAR (Same as Report). An entry in this block is necessary if the abstract is to be limited.

Int. J. Appl. Ceram. Technol., 7 [5] 616–624 (2010)
DOI:10.1111/j.1744-7402.2010.02508.x

International Journal of
Applied Ceramic TECHNOLOGY
Ceramic Product Development and Commercialization

Dynamic Ring-on-Ring Equibiaxial Flexural Strength of Borosilicate Glass

Xu Nie and Weinong W. Chen*

AAE and MSE Schools, Purdue University, West Lafayette, Indiana 47907-2045

Douglas W. Templeton

U.S. Army TARDEC, Warren, Michigan 48397-5000

A novel dynamic ring-on-ring equibiaxial flexural testing technique with single pulse loading capability is established on a modified Kolsky bar. This technique is then utilized to investigate the loading-rate and surface-condition effects on the flexural strength of a borosilicate glass. Quasi-static and dynamic experiments are performed at loading rates ranging from 5×10^{-1} to 5×10^{6} MPa/s. It is found that the flexural strength of the borosilicate glass strongly depends on the applied loading rates. HF acid corrosion on the surface promotes the flexural strength to above 1.3 GPa. Fractographic analysis shows that surface modification has changed the type of flaws that govern the flexural strength of glass samples.

Introduction

Research on transparent armor glasses and ceramics has received increasing attention due to their wide applications as vehicle windows. Experimental studies on several candidate materials under high strain rate compressive loading conditions have provided measures on the mechanical and failure behaviors of the materials.[1,2] However, more systematic research efforts are still needed to develop a complete understanding of the dynamic failure of the transparent armor materials. In the event of impact on a window plate, the dominant and vital failure is shown to be spalling and bending-induced tension on the back side of the plate.[3] Under such a loading condition, the plate material

Partially supported by the U.S. Army Research Office under Grant No. W911-05-1-0218 to Purdue University.
*wchen@purdue.edu

is subjected to an out-of-plane deflection in a biaxial stress state.

Over the past several decades, vast amount of research has been carried out to explore the biaxial flexural strength of glass and ceramic materials.[4–9] Together with these experimental efforts, theoretical and numerical analyses were proposed through statistical approach to better interpret the strength data and failure mechanisms.[4,7,10,11] However, it was only until recently that these studies have been expanded to dynamic loading conditions, for which the data are of great desire to the high speed impact applications. Cheng *et al.*[12] tested the dynamic biaxial flexural strength of a thin ceramic substrate with a modified piston-on-three-ball testing configuration. In these experiments, dynamic loading is applied on the center of the specimen through a thin incident bar driven by a force hammer. Because dynamic loading may induce resonance in the sample that superimposes inertia forces on the intrinsic material response, there is an upper limit in the loading rates. The highest frequency component in the loading pulse should be controlled to be lower than the first resonant frequency of the specimen.[13]

Except under extremely high pressure or temperature, the failure of brittle materials under impact is controlled by flaw nucleation, propagation, and coalescence. At a higher loading rate, more flaws need to be driven simultaneously to dissipate enough elastic energy upon fracture, which requires a higher load to fail the material and thus causes the rate dependence of the material strength. When the material under investigation is glass, in addition to rate effects, these materials are also susceptible to surface flaws due to the lack of bulk flaws.[14] Flexural tests on glass materials suggested that the shape and severity of surface flaws are the key factors in strength determination.[15,16] Consequently, the dynamic biaxial bending behavior of glass materials should be determined together with the loading-rate and surface-flaw effects.

In this paper, we studied the surface-flaw and loading-rate effects on the biaxial flexural strength of a borosilicate glass utilizing a modified Kolsky bar, also called a split Hopkinson pressure bar (SHPB), with its testing section customized into a ring-on-ring equibiaxial bending configuration. Pulse-shaping technique is applied on the Kolsky bar to ensure both force equilibrium and constant loading rate in the specimen. In order to preserve the fracture surfaces, a momentum trap is attached to the incident bar to prevent multiple loading on the sample resulting from stress wave reflections in the incident bar. Circular disk glass specimens used in this research are subjected to three different surface conditions: ground by 180-grit sandpaper, mechanically polished, and polished and etched by 5% HF acid. These surface treatments are intended to introduce/modify surface flaws such that the fracture mechanisms may be altered. Scanning electron microscopy (SEM) is used to characterize the features on the fracture surfaces.

It is found that the flexural strength of the borosilicate glass increases with increasing loading rates under all surface conditions. The HF acid etching promotes glass surface tensile strength by a factor of 4 under equibaxial bending, while sandpaper grinding compromises the strength by about 50% due to the severe surface flaws introduced by abrasive particles.

Experimental Procedures

Materials and Specimens

The borosilicate glass used in this research is provided by U.S. Army Research Laboratory, Aberdeen Proving Ground, MD, in the form of 3.3-mm-thick flat plates. The material composition and specifications can be found in a previous paper studying the shear-stress effects on the compressive strength of the same glass.[2] These glass plates were machined to disks of 2 mm in thickness and 45 mm in diameter, with the top and bottom surfaces being mechanically polished to 40/20 scratch/dig and the overall surface roughness to be <20 Å. In order to reduce the possibility of edge failures, the circumferences of the disks were fire polished to eliminate sharp surface cracks induced by grinding. The as-polished samples were then divided into three groups. The first group stayed at the original as-received state and was tested without further surface modifications. The second group of samples was ground by 180-grit sandpapers to intentionally introduce surface flaws. The last group was etched by 5 wt% of HF acid aqueous solution for 15 min. This specific modification is performed to either completely remove or significantly blunt the preexisting surface flaws by stripping off the glass surface layer by layer during etching. The etching process results in a 20-μm reduction in thickness at each surface of the samples. To avoid the possible moisture interaction with etched glass to inhibit the formation of new surface cracks, the etched specimens were subjected to mechanical loading within several minutes after etching.

Experimental Techniques

Strength Test Methodology: In our previous study,[17] uniaxial four-point bending tests were carried out on the same material with an in-house-made loading fixture in the testing section of a Kolsky bar. It was found that at a certain stress level, the fracture origins universally shifted from the central surface to the edge, presumably due to the competing failure mechanisms between surface flaws and edge flaws. However, with the interference of edge failure, the flexural strength measured in these tests are considered to be lower than the intrinsic surface tensile strength due to the fact that the stress on the edge is concentrated and does not reflect the global tensile stress on the surface. Therefore, a new flexural testing technique without the influence of edge flaws is desirable for the characterization of dynamic flexural strength of borosilicate glass when surface-located flaws are strength limiting. In this study, an equibiaxial ring-on-ring testing fixture was developed according to ASTM C1499,[18] and introduced to a modified Kolsky bar. A pair of concentric steel rings was attached to concentric aluminum substrates on the Kolsky bar so that the system alignment is secured. The rings were hardened to HRC 60 and then polished to ensure a smooth contact with glass samples. The diameters of these concentric rings were 12.5 and 25 mm, respectively, with a ring tip radius of 2.5 mm. The incident and transmission bars of the Kolsky-bar setup are made of 6061-T6 aluminum alloy with a common diameter of 31.75 mm. An image of this testing configuration is shown in Fig. 1. In addition to the ring fixture, a pair of universal joints that are of the same diameter as the bars was also placed between the gage section and the transmission bar. Universal joints were adopted in Kolsky-bar system to eliminate possible misalignment in the gage section.[19] This modification is very important in brittle material testing because these materials are susceptible to failure initiation from concentrated stresses. If the stress distribution in the specimen is nonuniform, premature failure may occur even when the global stress level is still low. The joints used in this research are composed of a convex plane and a concave plane, which are of equal curvature and facing each other. During specimen installation, this pair of surfaces is the last to engage, eliminating misalignment and ensuring an even contact between the loading rings and the specimen surface.

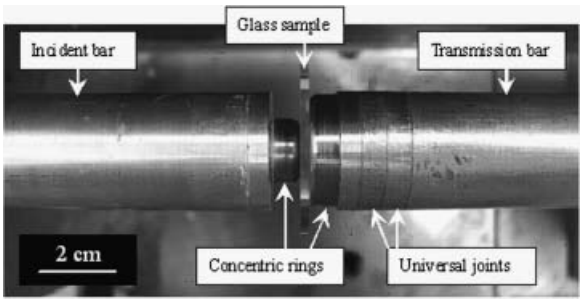

Fig. 1. Dynamic ring-on-ring test section configuration.

Dynamic experiments were carried out on a modified Kolsky-bar setup. Kolsky bar is a well-established experimental method utilized for the characterization of dynamic properties of materials over a large range of strain rates.[20] Originally developed by Kolsky,[21] this technique was initially proposed to characterize the stress–strain behavior of ductile materials at strain rates up to 10^4/s. Over the past decades, a growing desire to understand the dynamic properties of a broader range of materials has urged further modifications on this device. With the implementation of pulse shaping technique,[22] the application of this high strain rate testing device has been extended to the characterization of a variety of materials including soft materials[23] and brittle materials.[1,2] A pulse shaper is normally a thin disk of ductile metal placed on the impact end of the incident bar. For a given impact velocity, the shape and magnitude of the incident pulse can be adjusted by changing the diameter, thickness, and the material type of the pulse shaper. In a conventional Kolsky-bar experiment where pulse shapers were not used, the incident pulse profile is trapezoidal with high-frequency oscillations riding on the plateau. These high-frequency components not only make the stress state in the specimen complicated but also may cause the disk specimen to vibrate, leading to inaccurate stress/strain measurements. This makes the measured sample stress history uncertain. Therefore, to load the disk specimen at a nearly constant loading rate without exciting resonance, the loading pulse needs to be carefully designed and controlled in order to achieve a proper rise time and eliminate high-frequency components. In a ring-on-ring flexural experiment, the specimen loading rate is proportional to the deflection rate.[18] Hence, the profile of the loading pulse needs to be determined in such a way that the reflected wave (deflection rate history of the sample) has a plateau after the initial rise. In this study, an annealed copper disk pulse shaper of 1-mm-thick and 3.3 mm in diameter

was used to generate the desired incident ramp pulse at a resultant specimen loading rate of approximately 5×10^6 MPa/s.

Another modification for dynamic equibiaxial ring-on-ring test on glass materials is the single-pulse loading technique. In a quasi-static ring-on-ring experiment, the disk specimen is loaded at a certain deflection rate controlled by the crosshead speed. The end position of the crosshead can also be set so that the sample is loaded only by a well-defined loading profile. However, such a close-loop control system does not exist in a conventional Kolsky-bar setup. When the initial compressive wave arrives at the specimen end of the incident bar, part of the pulse is reflected back as a tensile wave due to the low wave impedance of the specimen compared with the incident bar. This tensile wave will again be reflected at the impact end of the incident bar as a secondary compressive wave, which reloads the sample. In this way, the specimen is loaded multiple times before the kinetic energy of the incident bar finally dissipates. Repeated loading on a fractured glass disk could activate additional failure sites at different locations, and encumber the fractographic analysis. In order to prevent the repeated compressive pulses from reloading the specimen, a momentum trapping technique has been adopted to ensure single loading on the specimen.[24] A brief illustration of this technique is shown in Fig. 2. A flange is screwed on the impact end of incident bar, with a heavy mass closely sitting against it. The heavy mass has a central hole that allows the incident bar to run through. The gap between the flange and heavy mass is calibrated such that after the first compressive wave passes through, the flange is in contact with the heavy mass. While the reflected tensile wave reaches the impact end to initiate the secondary compression, the heavy mass acts as a rigid wall and reverses the would-be compression pulse in the incident bar into a tension pulse. This tension pulse and its subsequent reflections pull the incident bar away from the specimen, thus leaving the specimen untouched after being loaded by the first incident pulse. The stress-wave signals in the incident bar with and without momentum trapping technique are compared in Fig. 3. It is clearly shown that with the momentum trapper, the secondary compressive wave is converted to a tensile wave, which eventually retracts the incident bar.

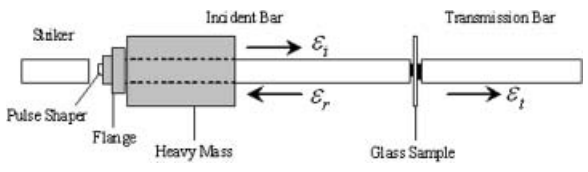

Fig. 2. Modified Kolsky bar with a momentum trapping system.

Quasi-static experiments were carried out on a servo-hydraulic testing machine with the same loading configuration as implemented in the Kolsky-bar setup. In both dynamic and quasi-static experiments, cellophane tape was applied to the compressive surface of the bending specimen to retain fracture fragments. The ring-specimen contact surfaces were lubricated by vacuum grease to minimize friction effects. The temperature of the testing environment was 26°C, with a relative humidity of 34%.

Fractography: Fractography was conducted on fracture surfaces to study the failure origins and types of surface flaws that initiated the fracture. Only the experiments where specimens failed within the loading ring

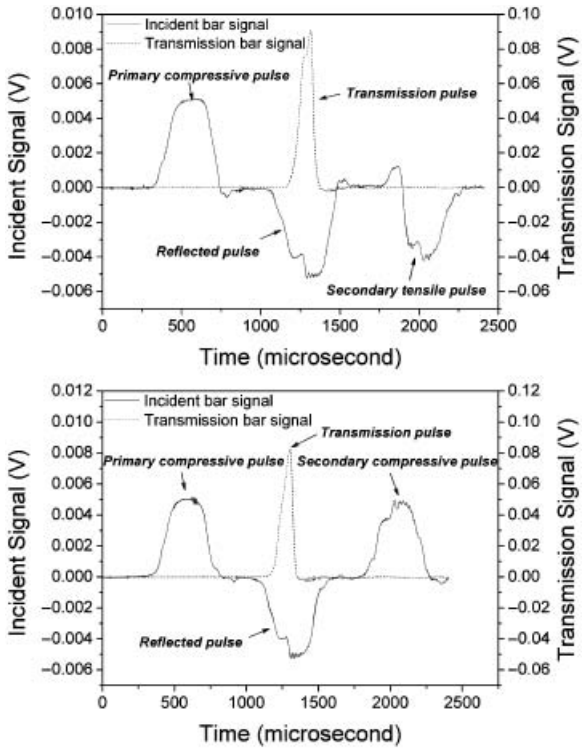

Fig. 3. Stress-wave signals in the incident and transmission bars (a) with a momentum trapper, and (b) without a momentum trapper.

area were considered to be valid tests. Radial fracture pattern of the fractured samples points to the location of failure initiation. The glass pieces were taken apart from the tape with extraordinary care to preserve the fracture surface. Optical microscopy was used to identify the exact failure origin on the fragments where the fracture was initiated. Selected fracture origins were further investigated by SEM to define the types of flaws.

Results and Discussions

Biaxial Flexural Strength

Equibiaxial flexural tests were conducted on all the three groups of glass samples at four loading rates (0.52, 42, 3500, and 5×10^6 MPa/s). The three lower rate experiments were performed on the servohydraulic machine, while the high rate experiments were conducted on the modified Kolsky-bar setup. The number of test specimens was chosen according to the specifications in ASTM C1499 such that at least 10 valid tests were secured at each loading rate and surface condition. A typical oscilloscope record from a Kolsky-bar experiment on an HF- acid-etched glass sample is shown in Fig. 4. The incident pulse is shaped into a nonlinear ramp to achieve a constant deflection rate in this acid-etched specimen before sample fracture. In a dynamic equibiaxial bending test, the glass specimen is initially subjected to acceleration until the desired loading rate is achieved. Under such conditions, the loading pulse profile needs to be carefully controlled in order not to excite the resonant frequency of the testing fixture; otherwise, a nonequilibrium force history will be imposed in the specimen in which the inertial force may be presented. In this study, the force histories on both loading-ring and supporting-ring sides were continuously monitored by the collected strain gage signals. Specifically, the force histories on the loading-ring side (F_L) and the force history on the supporting-ring side (F_S) are given by

$$F_L = EA(\varepsilon_i + \varepsilon_r) \quad (1)$$

$$F_S = EA\varepsilon_t \quad (2)$$

where E and A are Young's modulus and cross-sectional area of bars, respectively; ε_t is the strain history of transmitted pulse while ε_i and ε_r are the strain histories of incident and reflected pulses, respectively.

A typical dynamic force equilibrium check is shown in Fig. 5. As evident in the figure, the two force-history curves are in good agreement with each other during the entire loading period. The minor oscillations on both curves are presumably caused by stress-wave reflections in the ring-specimen testing section. Once dynamic force equilibrium is established, the biaxial flexural strength of the borosilicate-glass sample can be calculated by the peak load achieved in the sample in the light of the circular plate theory[25]:

$$\sigma_f = \frac{3F}{2\pi h^2}\left[(1-\nu)\frac{D_S^2 - D_L^2}{2D^2} + (1+\nu)\ln\frac{D_S}{D_L}\right] \quad (3)$$

where F is the peak load recorded, h is the thickness of the sample, D_S is the supporting-ring diameter, D_L is

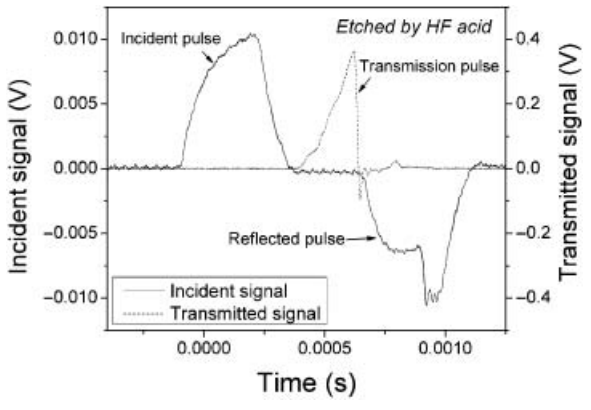

Fig. 4. Typical oscilloscope record from a Kolsky-bar experiment on a HF-acid-etched sample.

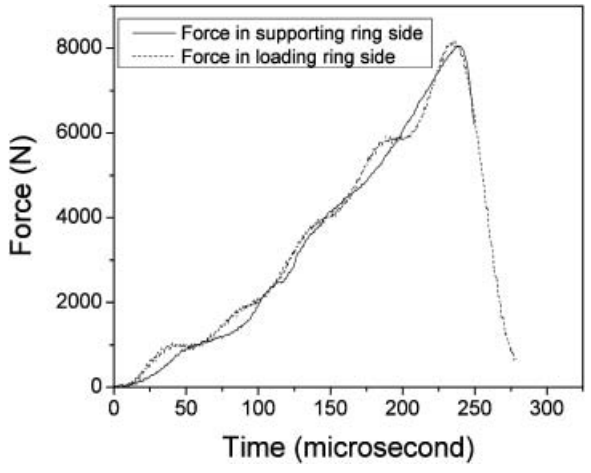

Fig. 5. Force equilibrium check in a dynamic ring-on-ring experiment.

Table I. Equibiaxial Flexural Strength of Borosilicate Glass under Different Loading Rates and Surface Conditions

Loading rate (MPa/s)	0.52	42	3500	5×10^6
HF etched (MPa)	352 ± 35.7	744 ± 96	1267 ± 124	1383 ± 137
As-polished (MPa)	146 ± 11	180 ± 13	245 ± 15	255 ± 19
Sandpaper ground (MPa)	46 ± 3	52 ± 4	77 ± 8	83 ± 7

Strength data are in MPa.

the loading-ring diameter, D is the diameter of the sample, and ν is Poisson's ratio of borosilicate glass.

The calculated strength values for borosilicate glass samples at different loading rates and surface conditions are summarized in Table I. The results indicate that the surface modifications significantly affect the flexural strength of the glass material. Sandpaper grinding degrades the strength by 60–70% from the as-polished surface condition. However, HF acid etching on as-polished specimens promotes the surface tensile strength by 200–400%, depending on the applied loading rates. The experimental results also indicate that the loading rate has remarkable effects on the flexural strength. Under all surface conditions tested, the strength universally increases with loading rates. But the rate of strength increase levels out at the loading rate of $\sim$3500 MPa/s.

Fractography

The strength variations observed under different surface conditions stimulated further fractography investigations to understand better the fracture mechanisms of borosilicate glass under equibiaxial flexural loading conditions. A series of fractured samples from Kolsky-bar experiments are shown in Fig. 6. Because the samples were loaded by a single pulse, the fragments were well preserved after the initial fracture events. As indicated by the fracture patterns shown in the figure, the likely failure origins are all located in the central areas of specimens regardless of surface conditions. No edge failure was identified in the study reported in this paper. It is also observed that the density of cracks increases with flexural strength due to the increasing amount of elastic energy that needs to be released during fracture. As for the sandpaper-ground samples, a primary crack (indicated by an arrow in Fig. 6a) is identifiable, while the other cracks were initiated at different locations along this crack. However, this primary crack becomes less distinct for the as-polished samples (Fig. 6b), on which the majority of cracks were converging back to a common origin. This crack pattern finally changed into a complete radiation type for the HF-acid-etched samples, with essentially all cracks converged back to exactly the same failure origin (shown in Fig. 6c). The transition in macroscopic cracking mode inspired further investigation on the strength-governing flaws under each surface condition. In this research, fracture surface images were taken by SEM and are shown in Fig. 7. It should be pointed out that, as can be seen from Fig. 6c, the equibiaxial bending fracture origin of HF-acid-etched sample is almost pulverized and thus the fracture surface around the failure-initiation flaw was heavily fragmented. For the purpose of comparison, SEM images showing the failure origins of an HF-acid-etched glass bar sample, which was loaded in four-point bending, are therefore given in Fig. 7c. For

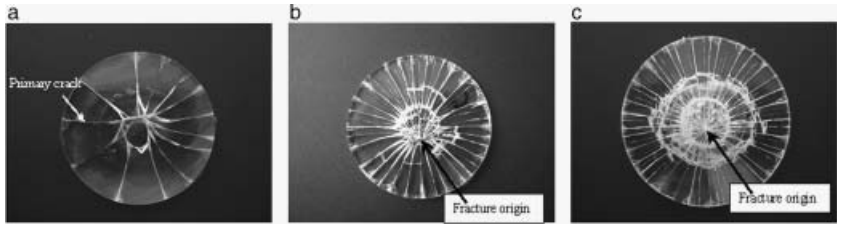

Fig. 6. Fracture mode of glass samples with different surface conditions (a) ground samples, (b) as-polished samples, and (c) acid-etched samples.

the sandpaper-ground samples, sharp cracks that penetrate into the subsurface are visible at the center of the fracture zone. Further polishing on the as-ground surfaces resulted in the reduction of critical crack size, and thus an increase in flexural strength. The strength governing the flaw size on HF-acid-etched surface is similar to that on the as-polished surface, whereas the flexural strength of the etched sample is four times higher than that of as-polished samples. The mechanisms of acid corrosion on glass surface were discussed by Proctor and colleagues.[26,27] It is assumed that there are sharp surface cracks existing on the machined and/or polished glass surfaces. During etching, the crack surfaces are uniformly attacked by HF acid at every point. Consequently, such a precrack develops into a semicircle or a semiellipse depending on the original crack shape and etching time (over etching would more likely lead to a semiellipse shape). A simultaneous acid attack on numerous surface cracks creates a ''bumpy'' surface pattern as is evident in Fig. 7c. According to the model, the final radii of these surface pits are determined by the depth of original flaws; hence, the observed variation in the pit radii may be directly related to the variation in initial crack size. The fracture surface of an etched sample reveals that failure was initiated at a severe surface pit. However, no sharp front of a precrack was identified.

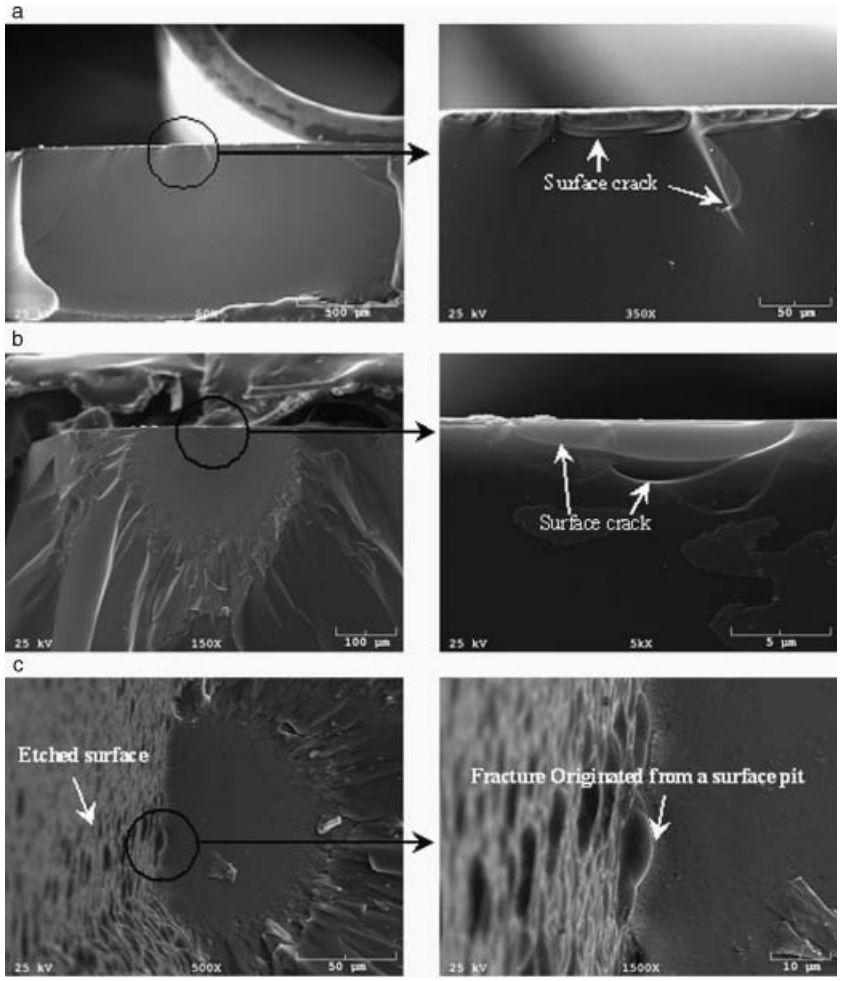

Fig. 7. Scanning electron microscopic images showing the fracture origins of glass samples receiving different surface modifications. (a) Ground by sandpaper, (b) As-polished, and (c) Polished and etched by HF acid. Fracture surfaces for acid-etched samples are taken from the four-point bending experiment for comparison purpose.

This indicates that the fracture of an etched specimen is originated from a blunt surface flaw, unlike the case of as-polished specimens where a sharp surface crack is located in the failure origin. As a result, although acid etching developed similar flaw depths possessed by as-polished samples, the blunt nature of etching pits offers much less stress intensity compared with the sharp crack front in polished samples, and thus raises the flexural strength significantly.

Slow Crack Growth (SCG)

Because all the tests were performed in ambient conditions, such a relationship between fracture strength and applied stress rate implies the SCG mechanism might have been activated. SCG is commonly found in flexural tests of ceramic materials, while the sample is loaded at relatively low stress rates, and is thought to be driven by the combination of applied stress and chemical composition in the test environment. For glass materials, water molecules in the atmosphere could react with silica bonds at the crack tip under the assistance of applied tensile stress (stress corrosion).[26] This reaction will lead to crack growth and thus the degradation of fracture strength. Flexural tests performed at very high stress rates or in an inert environment, however, typically do not exhibit SCG because either the experiment is too fast for the crack to grow or the absence of chemical compositions would inhibit the stress corrosion process. Therefore, the glass fracture strength first increases with the increasing stress rates but finally levels out at a certain transition stress rate. The rate dependence may be approximated by[28]

$$\sigma_f = [D\dot{\sigma}]^{1/1+n} \tag{4}$$

Taking the logarithm of Eq. (4), we obtain

$$\log \sigma_f = \left(\frac{1}{1+n}\right) \log D + \left(\frac{1}{1+n}\right) \log \dot{\sigma} \tag{5}$$

where σ_f is the fracture strength, $\dot{\sigma}$ is the applied stress rate, n and D are SCG parameters. Figure 8 shows the logarithm plot of fracture strength versus stress rate. According to Eq. (5), the SCG parameter can be determined by calculating the slope of the fitted line. Linear regression fit was only applied to the data points obtained from the three low-rate tests, because the highest rate (5×10^6 MPa/s) might have been beyond the region wherein the SCG mechanism is active. It needs to be pointed out that due to the limited number of glass

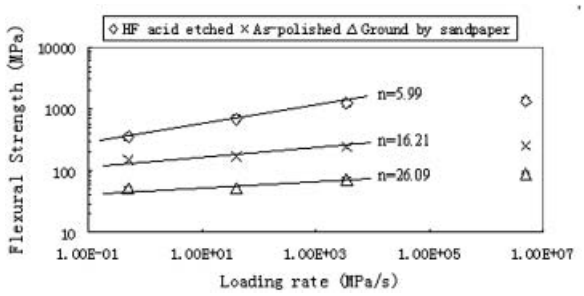

Fig. 8. Slow crack growth parameter determination for the low-rate tests. Solid line represents the best-fit line based on Eq. (5).

specimens, only 10 valid tests were conducted under each loading rate and surface conditions. Although this amount of tests is enough to characterize the mean biaxial strength of glass, it may not provide sufficient resolution to accurately scope the SCG behavior of borosilicate glass. Therefore, the SCG parameters obtained in this study may only provide a reference to our understanding on the stress corrosion process, which obviously has occurred during the course of experiments. As is evident from Fig. 8, the SCG parameter n appears to be a function of surface conditions, that is the initial flaw sizes. As the initial flaw size decreases, the material becomes more susceptible to SCG, which is indicated by the decreasing n value. Early study on stress corrosion has revealed that the diffusion rate of water molecules from atmosphere to the crack tip played an important role in crack growth under the assistance of applied stress.[29] This diffusion rate of water molecules, however, could be affected by many factors such as the relative humidity in the environment, the size of the flaw, the temperature, and the morphology of the crack. SEM images in Fig. 7 show the fracture surfaces of ground and as-polished samples consisting of similar flaw structures which are identified as sharp surface cracks induced by mechanical contact. The fracture surface of the etched samples, however, clearly shows the fracture originating from a surface pit that is blunt in nature, and sharp cracks may have developed underneath these pits upon mechanical loading. Although these pits are of a similar size to the crack origins in as-polished samples, they are completely different in terms of morphology. This difference may account for the significant difference in SCG parameters between these two surface conditions and would require future study for further confirmation.

Conclusions

A dynamic equibiaxial ring-on-ring flexural testing technique was established on a modified Kolsky bar. The sample was subjected to a controlled loading profile such that both a constant loading rate and dynamic force equilibrium were achieved during the entire loading period. In addition, single-pulse loading technique was adopted to ensure that the glass specimen was loaded only once and therefore in the fractography point of view, the fractured samples were as pristine as they were in a quasi-static experiment. This experimental technique was then applied to investigate the effect of different surface conditions and loading rates on the equibiaxial flexural strength of a borosilicate glass. Flexural strength of 1.3 GPa at dynamic loading rates was measured on specimens where the tensile surfaces were chemically etched by HF acid. The flexural strength of the borosilicate glass increases with increasing loading rates for all the surface conditions studied. SEM images on fracture surfaces showed that the as-polished and sandpaper-ground samples failed from the sites where sharp surface machining or grinding cracks were presented. The HF-acid-etched samples failed, however, from blunt semi elliptical surface pits, which were developed by a continuous acid attack.

Acknowledgement

The authors are truly grateful to Dr. Andrew Wereszczak for his insightful discussion and suggestions during this research.

References

1. B. Paliwalw, K. T. Ramesh, and J. W. McCauley, "Direct Observation of the Dynamic Compressive Failure of a Transparent Polycrystalline Ceramic (AlON)," *J. Am. Ceram. Soc.*, 89 [7] 2128–2133 (2006).
2. X. Nie, W. Chen, X. Sun, and D. Templeton, "Dynamic Failure of Borosilicate Glass Under Compression/Shear Loading," *J. Am. Ceram. Soc.*, 90 [8] 2556–2562 (2007).
3. A. S. Vlasov, E. L. Zilberbrand, A. A. Kozhushko, A. I. Kozachuk, and A. B. Sinani, "Behavior of Strengthened Glass Under High-Velocity Impact," *Strength Mater.*, 34 [3] 266–268 (2002).
4. R. A. Jeryan "Use of statistics in ceramic design and evaluation," *Proceeding of the 5th Army Materials Technology Conference*, Newport, RI, 1977.
5. D. K. Shetty, A. R. Rosenfield, G. K. Bansal, and W. H. Duckworth, "Biaxial Fracture Studies of a Glass-Ceramic," *J. Am. Ceram. Soc.*, 64 [1] 1–4 (1981).
6. D. K. Shetty, A. R. Rosenfield, W. H. Duckworth, and P. R. Held, "Biaxial-Flexural Test for Evaluating Ceramic Strengths," *J. Am. Ceram. Soc.*, 66 [1] 36–42 (1983).
7. B. J. de Smet, P. W. Bach, H. F. Scholten, L. J. M. G. Dortmans, and G. de With, "Weakest-Link Failure Predictions for Ceramics III: Uniaxial and Biaxial Bend Tests on Alumina," *J. Eur. Ceram. Soc.*, 10 101–107 (1992).
8. M. H. Krohn, J. R. Hellmann, D. L. Shelleman, and C. G. Pantano, "Biaxial Flexure Strength and Dynamic Fatigue of Soda–Lime–Silica Float Glass," *J. Am. Ceram. Soc.*, 85 [7] 1777–1782 (2002).
9. A. Borger, R. Danzer, and P. Supancic, "Biaxial Strength Test of Discs of Different Size Using the Ball on Three Balls Test," *28th Int. Conf. Adv. Ceram. Comp. B: Ceram. Eng. Sci. Proc.*, 25 [4] 283–288 (2004).
10. T. Thiemeier and A. Bruckner-Foit, "Influence of the Fracture Criterion on the Failure Prediction of Ceramics Loaded in Biaxial Flexure," *J. Am. Ceram. Soc.*, 74 [1] 48–52 (1991).
11. S. G. Reid, "Effects of Spatial Variability of Glass Strength in Ring-on-ring Tests," *Civil Eng. Environ. Syst.*, 24 [2] 139–148 (2007).
12. M. Cheng, W. Chen, and K. R. Sridhar, "Experimental Method for a Dynamic Biaxial flexural Strength Test of Thin Ceramic Substrates," *J. Am. Ceram. Soc.*, 85 [5] 1203–1209 (2002).
13. M. Cheng, W. Chen, and K. R. Sridhar, "Biaxial Flexural Strength Distribution of Thin Ceramic Substrates with Surface Defects," *Int. J. Solids Struct.*, 40 2249–2266 (2003).
14. M. Hara, "Some Aspects of Strength Characteristics of Glass," *Glastechnische Berichte*, 61 191–196 (1988).
15. J. E. Ritter and M. R. Lin, "Effect of Polymer Coatings on the Strength and Fatigue Behavior of Indented Soda–Lime Glass," *Glass Technol.*, 32 [2] 51–54 (1991).
16. J. J. Jr. Mecholsky, S. W. Freiman, and R. W. Rice, "Effect of Grinding on Flaw Geometry and Fracture of Glass," *J. Am. Ceram. Soc.*, 60 [3–4] 114–117 (1977).
17. X. Nie, W. Chen, A. Wereszczak, and D. Templeton, "Effect of Loading Rate and Surface Conditions on the Flexural Strength of Borosilicate Glass," *J. Am. Ceram. Soc.*, 92 1287–1295 (2009).
18. ASTM *Standard Test Method for Monotonic Equibiaxial Flexural Strength of Advanced Ceramics at Ambient Temperature. Annual Book of ASTM Standards C1499 – 05*, ASTM, West Conshohocken, PA, 2003.
19. W. Chen and H. Luo, "Dynamic Compressive Responses of Intact and Damaged Ceramics from a Single Split Hopkinson Pressure Bar Experiment," *Exp. Mech.*, 44 [3] 295–299 (2004).
20. G. T. Gray, "Classic Split Hopkinson Pressure Bar Technique," *ASM Handbook, Vol. 8, Mechanical Testing and Evaluation*. eds., H. Kuhn and D. Medlin. ASM International, Materials Park, OH, 462–476, 2000.
21. H. Kolsky, "An investigation of the mechanical properties of materials at very high rates of loading," *Proc. R. Soc. Lond.*, B6 676–700 (1949).
22. D. J. Frew, M. J. Forrestal, and W. Chen, "Pulse Shaping Techniques for Testing High-Strength Steel with a Split Hopkinson Pressure Bar," *Exp. Mech.*, 45 [2] 186–195 (2005).
23. B. Song and W. Chen, "Split Hopkinson Bar Techniques for Characterizing Soft Materials," *Lat. Am. J. Solids Struct.*, 2 113–152 (2005).
24. B. Song and W. Chen, "Loading and Unloading SHPB Pulse Shaping Techniques for Dynamic Hysteretic Loops," *Exp. Mech.*, 44 622–627 (2004).
25. S. P. Timoshenko and S. Woinowsky-Krieger, *Theory of Plates and Shells*, 2 nd edition, McGraw-Hill, New York, 1959.
26. B. A. Proctor, "Fracture of Glass," *Appl. Mater. Res.*, 3 28–34 (1964).
27. V. M. Sglavo, R. Dal Maschio, and G. D. Soraru, "Effect of Etch Depth on Strength of Soda–Lime Glass Rods by a Statistical Approach," *J. Eur. Ceram. Soc.*, 11 341–346 (1993).
28. S. R. Choi and J. A. Salem, "Ultra-fast Fracture Strength of Advanced Ceramics at Elevated Temperatures," *Mater. Sci. Eng. A*, 242 129–136 (1998).
29. S. M. Wiederhorn, "Influence of Water Vapor on Crack Propagation in Soda–Lime Glass," *J. Am. Ceram. Soc.*, 50 407–414 (1967).